Title

Restoring Visual Function to Blind Mice with a Photoswitch that Exploits Electrophysiological Remodeling of Retinal Ganglion Cells

Journal

Neuron, 81(4)

ISSN

0896-6273

Authors

Tochitsky, Ivan
Polosukhina, Aleksandra
Degtyar, Vadim E
et al.

Publication Date

2014-02-01

DOI

10.1016/j.neuron.2014.01.003

Peer reviewed

Published in final edited form as:
Neuron. 2014 February 19; 81(4): 800–813. doi:10.1016/j.neuron.2014.01.003.

Restoring visual function to blind mice with a photoswitch that exploits electrophysiological remodeling of retinal ganglion cells

Ivan Tochitsky[1], **Aleksandra Polosukhina**[2], **Vadim E. Degtyar**[1], **Nicholas Gallerani**[1], **Caleb M. Smith**[1], **Aaron Friedman**[3], **Russell N. Van Gelder**[4], **Dirk Trauner**[5], **Daniela Kaufer**[3,6], and **Richard H. Kramer**[1,2,6]

[1]Department of Molecular and Cell Biology, University of California, Berkeley, Berkeley, CA 94720, USA

[2]Vision Science Graduate Group, University of California, Berkeley, Berkeley, CA 94720, USA

[3]Department of Integrative Biology, University of California, Berkeley, Berkeley, CA 94720, USA

[4]Departments of Ophthalmology, Pathology and Biological Structure, University of Washington, Seattle, WA 98195, USA

[5]Department of Chemistry and Biochemistry, University of Munich, D-81377 Munich, Germany

[6]Helen Wills Neurosciences Institute, UC Berkeley, Berkeley, CA 94720, USA

Summary

Retinitis pigmentosa (RP) and age-related macular degeneration (AMD) are blinding diseases caused by the degeneration of rods and cones, leaving the remainder of the visual system unable to respond to light. Here we report a chemical photoswitch named DENAQ that restores retinal responses to white light of intensity similar to ordinary daylight. A single intraocular injection of DENAQ photosensitizes the blind retina for days, restoring electrophysiological and behavioral responses with no toxicity. Experiments on mouse strains with functional, non-functional, or degenerated rods and cones show that DENAQ is effective only in retinas with degenerated photoreceptors. DENAQ confers light sensitivity on a hyperpolarization-activated inward current that is enhanced in degenerated retina, enabling optical control of retinal ganglion cell firing The acceptable light sensitivity, favorable spectral sensitivity, and selective targeting to diseased tissue make DENAQ a prime drug candidate for vision restoration in patients with end-stage RP and AMD.

Introduction

Degenerative retinal diseases including AMD and RP affect millions of people around the world. At present, there are no effective treatments to prevent the progressive degeneration of rod and cone photoreceptors that characterizes these disorders. Without a means for restoring photoreception, patients with advanced RP face the prospect of irreversible blindness. Several technologies are being developed to confer information about the visual world to the retinal neurons that survive after the rods and cones have degenerated.

Correspondence: rhkramer@berkeley.edu.

Surgically implanted electronic retinal prosthetics can electrically stimulate RGC firing, restoring some visual perception to blind humans (Weiland et al., 2011). Transplantation of stem cell-derived photoreceptors can restore retinal light responses to blind mice (Lamba et al., 2009) and a retinal pigment epithelium transplant has improved vision in a patient with AMD (Schwartz et al., 2012). Viral expression of microbial opsins (Busskamp et al., 2010; Lagali et al., 2008; Thyagarajan et al., 2010) or other optogenetic tools (Caporale et al., 2011) can restore visual responses in blind mouse models of RP. All of these strategies have shown promise for restoring visual function, but they are either invasive (i.e. implantation of electronic chips) or irreversible (i.e. transplantation of photoreceptor progenitors or viral expression of optogenetic tools). The potential permanence of stem cell or gene therapies could be a benefit if complications are absent, but the possibility of irreversible adverse effects makes these interventions potentially risky to implement in humans.

We recently introduced another strategy for restoring visual function: adding a synthetic small molecule “photoswitch” to confer light sensitivity onto retinal neurons without involving exogenous gene expression. We showed that a photoswitchable K^+ channel blocker named AAQ could bestow light responses onto RGCs and restore light-elicited behavior in blind mice *in vivo* (Polosukhina et al., 2012). As a drug-like small molecule, AAQ has some potential advantages over the other approaches for vision restoration. Unlike microbial opsin or stem cell-based therapies, the effect of AAQ is reversible, allowing the dosage to be adjusted to maximize efficacy and minimize toxicity. Furthermore, photoswitch compounds diffuse freely and photosensitize neurons throughout the entire retina. This ensures broader coverage and higher spatial resolution than a retinal implant, which covers only a small area of the retina with stimulating electrodes that are spaced further apart than the packing density of RGCs.

Unfortunately, several properties of AAQ limit its potential for therapeutic development. AAQ requires high intensity, UV light and dissipates from the eye within a day after intravitreal injection. The human lens filters out most UV light (Artigas et al., 2012) and repeated exposure to high intensity light can be damaging (Noell et al., 1966). AAQ’s short half-life would necessitate daily injections of the compound into the eye, a delivery schedule unsuitable for long-term treatment. Furthermore, AAQ contains a reactive acrylamide moiety and its toxicity *in vivo* is unknown. In an attempt to overcome these shortcomings we have turned to a red-shifted K^+ channel photoswitch called DENAQ, which exhibits *trans* to *cis* photoisomerization with visible light (450–550 nm) and which relaxes rapidly to the *trans* configuration in the dark (Mourot et al., 2011).

Results

DENAQ restores photopic light responses to the degenerating mouse retina

DENAQ is a red-shifted photoswitch compound (Figure 1A) that confers light sensitivity on voltage-gated ion channels (Mourot et al., 2011; Mourot et al., 2013). We tested the action of DENAQ on the retinas of 3–6 month old *rd1* mice, which lose nearly all rods and cones within 1 month after birth (Sancho-Pelluz et al., 2008). We measured the effect of light on action potential firing by RGCs recorded with an extracellular multi-electrode array (MEA). Before photoswitch application, light caused no significant change in firing rate (Figure 1B). Treatment with 300 μM DENAQ for 30 min photosensitized the retina, such that nearly all RGCs responded to the onset of a 15 sec light flash with an increase in firing rate (Figure 1C). On average, DENAQ-treated RGCs generated a significant firing rate increase within ~20 msec of light onset ($p<0.05$), reaching their peak firing within 400 msec. Thereafter, the firing frequency declined during the flash. Azobenzene photoswitches reach a stable photostationary state with sustained illumination (Fischer et al., 1955), so the decline in firing rate is likely a consequence of spike frequency adaptation intrinsic to RGCs rather

than the photochemical properties of DENAQ. At light offset, the average firing rate across all units returned to baseline within ~600 msec, but >20% of units recovered within 100 msec. The decay of the DENAQ-mediated response at light offset is dependent on fast *cis* to *trans* thermal relaxation (Mourot et al., 2011), in contrast to AAQ, which persists in the *cis* state for >10 minutes and needs to be reset with green light (Fortin et al., 2008).

We next examined the spectral sensitivity of DENAQ-mediated photosensitization of the *rd1* retina. A wide range of wavelengths between ~400 to ~550 nm, can elicit the light response, with blue-green light (480–500 nm) being most effective in the visible range (Figure 1D). The action spectrum of retinal photosensitization closely matches the absorption spectrum of *trans*-DENAQ in solution (Mourot et al., 2011). Stimulation with broad spectrum white light is also effective. To quantify the degree of photosensitization for each RGC we calculated the Light Response Index (LRI) (previously designated the "photoswitch index" (Polosukhina et al., 2012)). The LRI is the normalized change in average firing rate upon switching from darkness to white light. RGCs from untreated *rd1* retinas showed no detectable light response (median LRI=0, n=12 retinas); while nearly all RGCs treated with DENAQ were activated by white light (median LRI=0.42, n=12 retinas, $p<0.001$, rank sum test) (Figure 1E). For every untreated retina studied, light caused no significant change in firing rate (n=12, p=0.94) (Figure 1F), while for every DENAQ-treated retina, light elicited a significant increase in firing rate (mean increase=2.4-fold, n=12, $p<0.001$) (Figure 1G).

The light intensity threshold for triggering RGC firing was 4×10^{13} photons/cm^2/sec for DENAQ (Figure 2A). More RGCs could be recruited to respond by increasing light intensity, with ~1 log unit above threshold (3×10^{14} photons/cm^2/sec) needed to generate a response in >50% of RGCs (Figure 2B). For comparison, the threshold for responses mediated by AAQ (Polosukhina et al., 2012), ChR2 expressed in RGCs (Thyagarajan et al., 2010) and halorhodopsin (NpHR) expressed in remnant cones (Busskamp et al., 2010) was 4×10^{15}, 1×10^{14}, and 2×10^{14} photons/cm^2/sec, respectively. Thus, the sensitivity of DENAQ-treated retinas is as high, if not higher, than that of retinas expressing these microbial optogenetic tools. New optogenetic tools with improved light sensitivity (Chow et al., 2010) are available, but have not yet been tested for vision restoration.

Photosensitivity can also be conferred to the *rd1* retina by injecting DENAQ into the vitreous cavity of eye *in vivo*. MEA recordings at later times after injection showed that DENAQ photosensitization persists for several days (half-life=2.1 days), in contrast to AAQ, which dissipates within 12 hours after intravitreal injection (half-life of 3.6 hours) (Figure 2C). The relative lifetime of the compounds in the eye mirrors their relative lipophilicity, with the more hydrophobic DENAQ persisting longer than AAQ.

We characterized the receptive field properties of DENAQ-treated RGCs. Illumination of the retina with a small spot of light resulted in an increase in activity in stimulated RGCs (median LRI=0.45, n=16 cells), but the surrounding unilluminated RGCs showing no change in firing rate (median LRI=−0.01, n=741 cells, $p<0.001$, rank sum test) (Figures 3A, 3B and Table S1). Since only targeted neurons near a single electrode showed a light response and since individual RGCs are detected by only one electrode on the MEA (which are spaced 200 μm apart), we can estimate that the DENAQ-mediated RGC collecting area is at most ~200 μm in diameter. Indeed, as we stimulated RGCs with expanding spots of light, the response increased with larger spot size and saturated at an average spot diameter of 240 μm (Figure 3C). No further increase in light response was observed with spot size greater than 240 μm or full field stimulation. The estimated receptive field size of DENAQ-treated RGCs matches previous measurements of mouse RGC dendritic fields, which average ~200 μm in diameter (Ren et al., 2010). Stimulation with small, 30 μm diameter

light spots was sufficient to drive RGC activity, suggesting that neighboring RGCs could, in principle, be manipulated independently with a precise stimulus, offering a basis for high-acuity vision. The receptive field properties are different in AAQ-treated retina, because chemical photosensitization extends to inhibitory amacrine cells, leading to an antagonistic center-surround response in RGCs (Polosukhina et al., 2012).

DENAQ selectively photosensitizes retinas with degenerated rods and cones

Photoreceptor degeneration in RP progresses from the peripheral to the central retina, which in some patients, can remain disease-free for years (Milam et al., 1998). In AMD, the pattern is reversed, with photoreceptor degeneration largely restricted to the central retina (Khandhadia et al., 2012). For any technology that restores photosensitivity, it would be preferable if the treatment selectively acted on diseased retinal regions while sparing healthy tissue. To assess the actions of photoswitch compounds on healthy and diseased retina, we compared the effects of DENAQ in wild-type (WT) vs. *rd1* retinas. The light stimulus parameters were the same as those shown in Figure 1. The WT retina is naturally sensitive to light, so not surprisingly almost all RGCs exhibited strong light responses with light-onset triggering an increase in firing in some neurons (ON-RGCs) and a decrease in others (OFF-RGCs) (Figure 4A). However, it was surprising to find that DENAQ treatment caused no change in the light response of the WT retina, with no difference in the number of RGCs generating On vs. Off responses (Figure 4B). To quantify this comparison, we calculated for each RGC the Peak Light Response Index (PLRI), which represents the normalized change in peak firing rate upon switching from darkness to light. Plotting the PLRI for each RGC reveals the distribution of neurons exhibiting primarily On- vs. Off- behavior (Figure 4C). We found no significant difference in the PLRI distribution before and after DENAQ treatment (n=6 retinas, p=0.34, rank sum test). Hence, at least according to this measure, DENAQ has no effect on the response properties of the wildtype retina, in stark contrast to its effect on the *rd1* retina.

The *rd1* retina differs from the WT retina in several ways. Not only have the rods and cones degenerated, which leads to changes in growth factor release (Amendola et al., 2003), but the neural circuitry of the retina no longer processes light-driven signals, which leads to homeostatic changes in synaptic transmission and neuronal excitability (Marc et al., 2003; Sekirnjak et al., 2011; Stasheff, 2008). To test whether the loss of light-driven signals is sufficient for enabling DENAQ photosensitization, we tested DENAQ on retinas from a triple knockout mouse (TKO) ($tra^{-/-}$ $cnga3^{-/-}$ $opn4^{-/-}$). The TKO mouse has the normal complement of structurally intact rods and cones, but light responsiveness in these cells has been impaired because of the loss of essential phototransduction proteins (Hattar et al., 2003). Also lacking is melanopsin, the photopigment of intrinsically photosensitive RGCs. As expected, TKO retinas did not respond to white light stimulation. But the retinas remained unresponsive even after DENAQ treatment (n=6 retinas, p=0.21, rank sum test) (Figure 4D). The lack of photosensitization suggests that the mere presence of intact photoreceptors, even if they are not light-sensitive, is sufficient to prevent DENAQ action.

We further tested the role of rod and cone degeneration in DENAQ photosensitization, by evaluating the effectiveness of the photoswitch in a different mouse model of RP. *Rd4* mice have a null mutation in rod transducin (Kitamura et al., 2006), whereas *rd1* mice suffer from a null mutation in rod phosphodiesterase (Bowes et al., 1990). The rods and cones degenerate soon after birth in both of these mouse strains, leading to complete blindness by 6 weeks of age (Roderick et al., 1997; Sancho-Pelluz et al., 2008). As expected, untreated retinas from 3–6 month old *rd4* mice did not generate a light response, but DENAQ treatment did confer robust light responses (n=6 retinas, p<0.001, rank sum test) (Figure

4D), just like in the *rd1* retina. Thus, it seems that rod and cone degeneration itself, and not any particular mutation, is what enables DENAQ photosensitization.

Mechanism of degeneration-specific photosensitization by DENAQ

In animal models of RP, the degeneration of rods and cones leads to an increase in the spontaneous firing rate of RGCs (Sekirnjak et al., 2011; Stasheff, 2008). The mechanism of this electrophysiological remodeling is unknown, but at least part of the hyperactivity is intrinsic to the RGCs themselves (Sekirnjak et al., 2011). To test whether RGCs are a target for DENAQ in degenerating retina, we applied a cocktail of neurotransmitter antagonists onto DENAQ-treated retinas to block glutamate, GABA, acetylcholine and glycine-mediated synaptic transmission. Under these conditions, RGCs continued to generate an increase in firing frequency in response to light (mean LRI=0.70, n=8 retinas) (Figures 5A and 5C). In fact, rather than being reduced by synaptic blockade, the light response of RGCs was increased, mainly due to a reduction in spontaneous firing in the dark. Similar results were obtained from RGCs in DENAQ-treated *rd4* retinas, which also continued to show light responses after synaptic blockade (mean LRI=0.43, n=6 retinas) (Figure 5C). Control experiments showed that the cocktail completely eliminated light-elicited changes in RGC firing mediated by normal rod and cone phototransduction in WT retina (Figure S1), confirming that blockade of retinal synaptic transmission was effective (Wong et al., 2007).

In contrast to the effects on degenerating retina, DENAQ failed to photosensitize pharmacologically-isolated RGCs in WT retinas (mean LRI=−0.01, n=10 retinas) (Figures 5B and 5C) and in retinas from TKO mice (mean LRI=0, n=6 retinas) (Figure 5C). Hence, while RGCs from degenerated retinas are strongly photosensitized by DENAQ, RGCs from intact retinas are DENAQ-insensitive. These results indicate that the primary cellular locus for DENAQ photosensitization is the RGC. This is different from AAQ photosensitization, which is mediated primarily by amacrine cells (Polosukhina et al., 2012).

We explored differences between *rd1* and WT retinas that might account for degeneration-specific DENAQ photosensitization. It seemed possible that DENAQ might have greater access to RGCs in degenerating retina, perhaps due to changes in the integrity or permeability of the inner limiting membrane (ILM) or outer limiting membrane (OLM). To test whether the ILM or OLM act as a barrier to prevent DENAQ photosensitization, we disrupted both membranes in the WT retina with a series of transverse cuts made by a sharp razor blade. Subsequent DENAQ treatment of these retinal slices failed to produce any photosensitization (mean LRI=0.03, n=6 retinas, p=0.62) (Figure S2). This experiment indicates that poor accessibility cannot account for the DENAQ-insensitivity of the WT retina.

Since DENAQ access is not the issue, perhaps the selectivity of DENAQ for the degenerating retina is caused by a change in conductances photosensitized by DENAQ. To compare the photosensitization of ionic conductances in WT and *rd1* RGCs, we obtained whole-cell patch clamp recordings after DENAQ treatment. We used the same cocktail of receptor antagonists to eliminate synaptic transmission, thereby revealing light-elicited effects on intrinsic conductances. Membrane potential was held at −60 mV and a series of test pulses from −100 mV to 0 mV were delivered to activate voltage-gated channels. Figures 6A–6C compare the current-voltage relationships of representative WT and *rd1* RGCs, and Figure 6D shows average data from all WT and *rd1* RGCs. In the RGC from the WT retina, light resulted in a small increase in the outward current elicited by depolarization above −40 mV, consistent with photoregulation of voltage-gated K^+ current (I_K) (Figures 6A, 6C and S3A). On average, light elicited a 15% increase in I_K (Figure 6D). However, light had no effect on ionic current near the resting potential (−70 mV) nor on the

hyperpolarization-activated current, I_h, elicited by steps to −100 mV (Figures 6A, 6C, 6D, S3A).

In contrast, in the RGC from the *rd1* retina, DENAQ conferred light sensitivity on ion channels that were active at both depolarized and hyperpolarized membrane potentials (Figures 6B and 6C). At potentials positive to −40 mV, light resulted in an increase in I_K, not significantly different from the effect of DENAQ on WT RGCs (Figure 6D; mean increase=23%, p=0.2). However, unique to the *rd1* cell, light also increased I_h (Figures 6B, 6C and S3B). On average, light increased I_h by ~20% in 11 RGCs tested (Figure 6D; p<0.001). At membrane potentials below −50 mV, light caused a steady inward current that would depolarize the cell, if it was not voltage-clamped. The light-regulated current increased non-linearly between −50 mV and −100 mV, consistent with the properties of I_h previously described in many neurons, including RGCs (Lee and Ishida, 2007; Stradleigh et al., 2011). A comparison of the light-elicited currents in WT and *rd1* RGCs (Figure 6D) shows that DENAQ only affects I_h in *rd1* RGCs. We propose that light-elicited enhancement of I_h is the primary cause of light-elicited RGC firing.

RGCs from *rd1* retina have a more depolarized average resting potential and a higher basal firing rate in darkness than RGCs from WT retinas (Figures 6A, 6B and (Stasheff, 2008)). We found that the current density of I_h is significantly larger in *rd1* RGCs (6.4 pA/pF) than in WT RGCs (2.9 pA/pF, p<0.01) (Figure 6E), consistent with enhanced excitability. However, the ~2-fold increase in current density seems insufficient to fully account for the dramatic difference in the light response, suggesting that there are additional differences in the properties of channels underlying I_h in *rd1* RGCs. I_K is slightly larger in *rd1* RGCs, but the difference from WT RGCs is not statistically significant (p=0.3).

To confirm that photosensitization of I_h mediates the DENAQ light response, we obtained MEA recordings from *rd1* retinas treated with three different I_h inhibitors. The light response was completely eliminated by ZD7288 (100 μM), a widely-used blocker of I_h (Postea and Biel, 2011). However, this blocker reduced the basal firing rate of RGCs in darkness (Figure 6F) and is known to inhibit certain voltage-gated Na^+ channels (Wu et al., 2012). Therefore we used two other blockers, ivabradine (50 μM) and cilobradine (50 μM), which are more specific for I_h (Postea and Biel, 2011) and do not noticeably decrease basal RGC activity (Figure 6F). Both of these drugs completely eliminated the DENAQ-mediated light response (Figures 6F and 6G). Similar results were obtained in DENAQ-treated retinas in the absence of synaptic blockers (Figure S4). Hence blockade of DENAQ-mediated photosensitization by I_h inhibitors is independent of changes in RGC excitability.

DENAQ is non-toxic

In order to assess the safety of DENAQ *in vivo*, we performed a histological analysis of WT retinas at 10 and 30 days post injection (DPI) of phosphate buffer saline (PBS) alone (sham) or PBS containing 5 mM DENAQ. No pathological changes were observed in either the DENAQ-injected or sham-injected retinas (Figure S5A). To determine whether DENAQ caused apoptosis of retinal neurons, we performed a TUNEL assay, which stains cells with nicked DNA, a marker of apoptosis (Loo, 2011). Apoptotic cells were extremely rare (<0.2%) (Figures S5A and S5B) and did not significantly differ in number between DENAQ and sham injected retinas (p_{10day}=0.16, p_{30day}=0.13). In contrast, DNase I treated retinas displayed extensive apoptosis, with 70% of retinal neurons staining positive in the TUNEL assay (Figures S5A and S5B). There was no significant difference between sham and DENAQ treated retinas in the thickness of the outer nuclear layer (p_{10day}=0.92; p_{30day}=0.77) or the inner nuclear layer (p_{10day}=0.39, p_{30day}=0.73) (Figure S5C). Finally, there was no change RGC density (cells per 100 μm) in the central (p=0.62) or peripheral retina (p=0.1) (Figure S5D).

DENAQ enables innate and learned behavioral light responses in blind mice

We next evaluated the ability of DENAQ to restore light-elicited behavior *in vivo*. Blind *rd1* mice showed no difference in exploratory behavior during 5 minutes spent in green light versus 5 minutes in darkness in an open field locomotory assay (Figures 7A and 7B). Six hours after intravitreal injection of DENAQ, individual mice displayed an increase in locomotory activity in light as compared to darkness (Figures 7A and 7B). Before DENAQ treatment the average velocity of movement for 20 mice tested was the same in darkness as in light, whereas after treatment their movement was faster in light than darkness (Figure 7C). The greatest increase in exploratory behavior was observed in the first 100 seconds of the light (mean ratio=1.74, n=20, $p<0.001$) (Figure 7C) and then diminished at later time points, most likely due to habituation. This increase in light-elicited locomotion is consistent with previously reported results from *rd1* mice expressing ChR2 in ON-bipolar cells (Lagali et al., 2008). Sham injection of PBS produced no significant change in basal activity or relative activity in light versus darkness (n=6, p=0.88) (Figure 7C).

Whatever vision restoration technology is ultimately employed, regaining normal sensory perception, including visual object recognition, will almost certainly require learning. To test whether *rd1* mice can use the DENAQ-mediated light response as a stimulus for a learned behavior, we used a visual-cued fear conditioning assay. In normally sighted mice, this classical conditioning paradigm associates a light cue with an electric foot shock, such that subsequent exposure to the light stimulus alone elicits a learned fear response (“freezing” behavior) (Li et al., 2012). We used 3 groups of animals for these studies: WT mice and *rd1* mice injected with either DENAQ or sham at 6 hours before training. On day 1 (training day), we exposed animals to either paired (3 trials of 10 s light stimuli, each co-terminating with a 2 s shock) or unpaired stimuli (the same light and shock stimuli interleaved rather than overlapping). On day 2 (recall day), we presented the light stimulus alone (Figure 8A). Sample recall trial movement traces of individual sham-injected *rd1* mice (left, black), DENAQ-injected *rd1* mice (middle, blue) and WT mice (right, red), all of whom had been exposed to paired conditioning during day 1, are shown in Figure 8B. WT mice that had received paired stimuli showed a decrease in locomotor activity in response to light on recall day (n=10, $p<0.001$) (Figures 8B and 8C). In contrast, sham-injected *rd1* mice showed no change in locomotor activity in response to light (n=9, p=0.98) (Figures 8B and 8C). However, DENAQ-injected *rd1* mice that had received paired conditioning showed a decrease in locomotor activity (i.e. freezing) in response to light (n=10, $p<0.001$), to the same extent as conditioned WT mice (n=10, p=0.51) (Figures 8B and 8C). DENAQ-injected *rd1* mice that had received unpaired stimuli showed no change in locomotor activity in response to light. These results demonstrate that the light perception conferred by DENAQ allows for visual learning, first enabling mice to associate light with a fearful stimulus on day 1, and then mediating the recall of the memory on day 2.

Discussion

DENAQ as a potential treatment for degenerative blinding disease

DENAQ has none of the serious shortcomings exhibited by AAQ. DENAQ has a red-shifted absorbance spectrum and therefore photoisomerizes from *trans* to *cis* with light in the 400–550 nm range, instead of the UV light required by AAQ. DENAQ photosensitizes the blind *rd1* retina to moderately bright white light, similar in intensity to ordinary daylight. The compound lasts in the eye for days following a single intravitreal injection. TUNEL staining and histological analyses show no evidence of adverse effects on the mouse retina. These features make DENAQ a favorable photoswitch candidate for preclinical development as a potential therapeutic for human use. Additional studies will be needed to assess acute toxicity potential in large mammals having eyes that are structurally and functionally closer

to humans. Both safety and efficacy of photosensitization can be assessed in several animal models of RP including blind strains of dogs (Petersen-Jones, 2005) and pigs (Li et al., 1998). There are no suitable primate models of RP, but laser ablation of photoreceptors can generate local scotomas that have features in common with human blinding disease (Hunter et al., 2012).

We delivered DENAQ *in vivo* by injecting it into the vitreous cavity of the eye. Intravitreal drug administration in humans has become commonplace. For example, anti-angiogenesis drugs for AMD are often administered in monthly injections (Comparison of Age-related Macular Degeneration Treatments Trials Research et al., 2012), which have proven to be safe (Ladas et al., 2009). DENAQ persists in the eye for up to a week after a single injection. A slow release formulation involving biodegradable polymer encapsulation (London et al., 2011) may extend the release lifetime of DENAQ to enable less frequent treatments (perhaps monthly) to sustain photosensitization.

Nonetheless, the transient nature of DENAQ photosensitization could be advantageous for minimizing possible adverse effects. The impermanence would allow for adjustment of dosage in individual patients to optimize vision restoration outcomes. In addition to potentially restoring visual function to end-stage RP patients with no light perception, DENAQ might be useful for enhancing visual performance in low vision patients with advanced RP or AMD. Moreover, acute RGC photosensitization with DENAQ might be useful for evaluating the functional integrity of the visual system in the brain before employing more permanent therapies, such as retinal implants.

Our results demonstrate that DENAQ can restore innate and learned visual behavioral responses in blind mice. We do not know whether these mice are capable of visually recognizing objects, but object recognition has not yet been demonstrated for any vision restoration technology implemented in blind mice. It is likely that whatever technology is used, training will lead to improvement in visual performance over time. Object recognition in human RP patients receiving a retinal implant improves dramatically with training (Humayun et al., 2012), similar to the progressive improvement of hearing of profoundly deaf patients outfitted with cochlear implants (Stacey et al., 2010). It is thus encouraging that light perception conferred by DENAQ is sufficient for visual learning and recall in blind mice.

Ideally, vision restoration technologies should enable the blind retina to respond to acceptable light intensities with sufficiently rapid kinetics to enable detection of moving objects. The kinetics of DENAQ-mediated responses are dependent on light intensity, with bright light maximizing the speed of response onset to less than 50 ms, and dim light allowing reliable responses to more frequent flashes. Spontaneous relaxation of DENAQ from *cis* to *trans* in darkness ($t_{1/2}$) takes ~300 ms (Mourot et al., 2011), consistent with the DENAQ-mediated RGC light response decaying within 1 sec, on average. However, the response kinetics vary considerably and some RGCs consistently turn off much quicker (<50 ms). In part, the speed of movement detection will depend on how the visual system weighs these different RGC responses. Novel azobenzene derivatives with nanosecond thermal relaxation kinetics have been developed (Garcia-Amoros et al., 2012) and photoswitches incorporating these compounds may enable very high frequency optical stimulation of neuronal firing.

The RGCs of DENAQ-treated blind mice all generate the same polarity light response, in contrast to the dual On vs. Off light responses generated by RGCs in normal functioning retinas, but this should not be a serious problem for visual perception. In human RP patients, electronic retinal implants can restore object recognition, even though the implants

indiscriminately stimulate On- and Off-RGCs (Humayun et al., 2012). DENAQ might enable some degree of visual perception under real-world photopic illumination conditions. However, image-altering projection goggles could improve perception by tuning the intensity, wavelength, refresh rate, and image complexity to optimize the visual experience.

Implications of degeneration-specific photosensitization

DENAQ has a profound effect on photoreceptor-degenerated retinas from *rd1* or *rd4* mice, while having little or no effect on healthy retinas from WT or TKO mice. The degeneration-dependent action suggests that DENAQ might selectively impart photosensitivity when cell death is constrained to a particular region, e.g. the peripheral retina in RP or the central retina in AMD. Our results imply that DENAQ will not interfere with normal phototransduction and visual processing in regions of the retina that are still healthy. The selective targeting of photosensitization to diseased tissue could be an important clinical advantage.

Our experiments indicate that RGCs are the primary cellular target for DENAQ photosensitization in the retina. The DENAQ-mediated light response is fully retained in RGCs after blocking all synaptic transmission, indicating that bipolar and amacrine cells are not required. We previously showed that the dominant cell type for AAQ-mediated photosensitization is the amacrine cell (Polosukhina et al., 2012). Light relieves AAQ blockade of K^+ channels in amacrine cells, hyperpolarizing the membrane potential, but because amacrine cells are inhibitory, the net effect is to enhance RGC firing. There are possible advantages in converting RGCs into the direct transducers of light input, rather than relying on presynaptic neurons to transmit this information. In principle, the latency of signaling to the brain will be shorter with direct RGC stimulation. And the signal generated directly in RGCs is downstream of retinal circuit remodeling that occurs during degeneration (Jones et al., 2012; Marc et al., 2003), which could distort spatial representation of images.

Our results indicate that degeneration of rods and cones in the outer retina somehow leads to changes in the electrophysiology of RGCs in the inner retina, enabling DENAQ photosensitization. We do not know whether the change in RGCs is triggered by the loss of light-driven synaptic input or trophic factor signaling. Morphological and electrophysiological changes in RGCs, resulting from degeneration, have been reported (Jones et al., 2012; Marc et al., 2003; Sekirnjak et al., 2011), but our results point to a previously unrecognized change in I_h as being the crucial alteration that enables DENAQ photosensitization.

I_h is a hyperpolarization-activated inward current that generates rebound depolarization after spikes, sustaining repetitive activity in cardiac myocytes and neurons (Lewis and Chetkovich, 2011). Our results show a ~2-fold increase of I_h in *rd1* RGCs, helping to explain why these neurons are hyperactive in degenerating retina. However, it is unclear whether the increase in current density alone accounts for the enormous increase in DENAQ photosensitivity, or whether additional changes in channel properties are involved. There are four hyperpolarization-activated cyclic nucleotide-gated (HCN) channel subunits, HCN1–4, that underlie I_h in different cell types (Lewis and Chetkovich, 2011; Postea and Biel, 2011). RGCs normally express HCN1 and HCN4 (Stradleigh et al., 2011) and both of these channels can be photosensitized by DENAQ when expressed as homomultimers in HEK-293 cells (unpublished observations). In addition to changes in channel expression, it is possible that a change in HCN channel localization, subunit composition or a change in auxiliary subunits, such as TRIP8b (Santoro et al., 2009) might alter the sensitivity of I_h to DENAQ.

DENAQ photosensitizes I_h and voltage gated K^+ channels in RGCs from *rd1* retina. Unlike K^+ channels, which are found in virtually every cell type in the eye, HCN channels are highly restricted to neurons (Müller et al., 2003). Different azobenzene photoswitches have overlapping but distinct selectivities for voltage-gated ion channels (Mourot et al., 2013). Thus, it may be possible to engineer a photoswitch compound that is specific for I_h, either by modifying chemical moieties in DENAQ, or by adding a light-sensitive azobenzene to a selective HCN ligand, such as ivabradine. A photoswitch specific for I_h would have the advantage of enabling photoregulation of neurons while having no effect on other cell types. By targeting I_h we have uncovered a new strategy for restoring visual function, based on exploiting changes in the endogenous electrophysiology of neurons that have remodeled during the progression of retinal degeneration.

Experimental Procedures

Chemicals

Photoswitch compounds were synthesized as formate salts in accordance with previously described protocols (Fortin et al., 2008; Mourot et al., 2011). All other chemicals were purchased from Sigma-Aldrich or Tocris Bioscience.

Animals

WT mice (C57BL/6J strain, Jackson Laboratory), homozygous *rd1/rd1* mice (C3H/HeJ strain, Charles River Laboratories), heterozygous *rd4/+* mice (In56Rk-*Rd4* strain, Jackson Laboratory) and triple knockout mice ($tra^{-/-}$ $cnga3^{-/-}$ $opn4^{-/-}$, gift of King-Wai Yau, Johns Hopkins University) 3–6 months old were used in the MEA experiments. All animal use procedures were approved by the UC Berkeley Institutional Animal Care and Use Committee.

Multielectrode array electrophysiology

Retinas were dissected and kept in physiological saline (ACSF) at 37°C containing (in mM) 119 NaCl, 2.5 KCl, 1 KH_2PO_4, 1.3 $MgCl_2$, 2.5 $CaCl_2$, 26.2 $NaHCO_3$, and 20 D-glucose, aerated with 95% O_2 / 5% CO_2. A solution containing (in μM) 10 AP4, 40 DNQX, 30 AP5, 10 SR-95531 (GABAzine), 50 TPMPA, 10 strychnine, 50 tubocurarine was used to pharmacologically isolate RGCs from outer retinal synaptic inputs,. For extracellular recordings, a flat-mounted retina, or a series of 400 μm wide transverse retinal sections made with a sharp razor blade, were placed ganglion cell layer down onto a multielectrode array system (MEA 1060-2-BC, Multi-Channel Systems). The MEA electrodes were 30 μm in diameter, spaced 200 μm apart and arranged in an 8×8 rectangular grid. Retinas were treated with 300 μM DENAQ in the MEA chamber for 30 min, followed by a 15 min wash. In order to pharmacologically isolate RGCs, the synaptic blocker cocktail (in ACSF) was subsequently perfused for 15 min. I_h was blocked by a 30 min perfusion of 100 μM ZD7288, 50μM ivabradine, or 50μM cilobradine (in ACSF with or without synaptic blockers). Extracellular spikes were high-pass filtered at 200 Hz and digitized at 20 kHz. A spike threshold of 4SD was set for each channel. Typically, each electrode recorded spikes from one to three RGCs. Principal component analysis of the spike waveforms was used for sorting spikes generated by individual cells (Offline Sorter, Plexon).

Patch-clamp electrophysiology

Borosilicate glass electrodes with resistance of 4–6 MΩ were used for all voltage clamp recordings. Access resistance was 5–14 MΩ. For measuring voltage-gated I_h and K^+ currents, electrodes contained (in mM) 116 K^+ gluconate, 6 KCl, 2 NaCl, 20 HEPES, 0.5 EGTA, 4 ATP-Mg, 0.3 GTP-Na_2, 10 Phosphocreatine-Na_2. The ACSF solution was the

same as the one used in the MEA experiments. Flat-mounted retinas were treated with 200 μM DENAQ for 40 min in ACSF at 25°C, followed by a 15 min wash. Synaptic inputs were blocked with a solution containing the same synaptic blockers as those used in the MEA experiments in addition to 1μM TTX-citrate. Current amplitudes for I-V relationships were measured as averages over 50ms at the end of voltage test pulses applied from the holding potential V_h=−60mV to −100mV, then stepping up to 0mV in 10mV increments every 1s. Two sets of I-V measurements were made in the dark and under 480nm light and averaged to calculate percent change in current. Photoregulation of I_h was quantified at −100mV and photoregulation of I_K at 0mV.

Light Stimulation

A 100W arc lamp (Ushio USH-103D) was used for MEA light stimulation. The photon flux equivalent for DENAQ-treated retinas was calculated using 470 nm (photoswitch absorbance peak) photon energy. The incident white light intensity for *rd1*, WT and TKO retinas was 3.3×10^{15} photons/cm^2/sec, and 3×10^{14} photons/cm^2/sec for *rd4* retinas, unless stated otherwise. AAQ-treated retinas were stimulated with filtered 380 nm and 500 nm light from the same lamp using narrow-band filters (Chroma, Inc), with the same light intensity as previously described (Polosukhina et al., 2012). A Polychrome V (Till Photonics GmbH) monochromator was used to determine the action spectrum of DENAQ in the retina. The action spectrum was corrected for photon flux at each individual wavelength. The Polychrome was also used to deliver 3.6×10^{15} photons/cm^2/sec of 480nm light to RGCs in patch clamp experiments. A typical MEA stimulation protocol consisted of 10 cycles of alternating 15 sec light/dark intervals.

Data Analysis and Statistics

We calculated the average RGC firing rate for individual retinas in light and in darkness in some experiments. In order to normalize light-elicited changes in firing rate of individual RGCs in *rd1*, *rd4* and TKO retinas, we calculated the LRI = (mean firing rate in the light – mean firing rate in darkness) / (mean firing rate in the light + mean firing rate in darkness). Light-elicited changes in firing rate of individual RGCs in WT retinas were calculated as PLRI = (peak firing rate in the light – peak firing rate in darkness) / (peak firing rate in the light + peak firing rate in darkness). The first second of the light and dark intervals was used to measure the peak firing rate. Pairwise comparisons of LRI and PLRI distributions were performed using the Wilcoxon rank sum test (Matlab). All other statistical significance (p value) calculations were performed using the two tailed unpaired Student's t test. Results with $p<0.05$ were considered significant.

Intravitreal injections

Before injection, animals were anesthetized with isoflurane (2%) and their pupils were dilated with tropicamide (1%). An incision was made through the sclera, below the ora serrata with a 30 gauge needle and 2 μL of either DENAQ (2 μL of various concentrations of DENAQ in 90% PBS / 10% DMSO) or vehicle only (sham) (2 μL of 90% PBS / 10% DMSO) were injected into the vitreous with a blunt ended 32 gauge Hamilton syringe. The mice were allowed to recover for 6 hours after injection with open access to food and water in their cage.

Cryosections

WT mice were euthanized by CO_2 asphyxiation and cervical dislocation 10 or 30 days after intravitreal injection. For each mouse, one eye was injected with 5mM DENAQ, while the other eye was injected with sham. For retinal cross sections, the animals were enucleated, the cornea and lens were removed, and the resulting eye-cups were fixed in 4%

paraformaldehyde for 1 hour at room temperature. The tissues were then cryoprotected in 30% sucrose overnight at 40C and frozen in OCT compound (Tissue-TEK, Sakura) with dry-ice ethanol slurry. Retinal sections were cut (15 μm) with a Microm HM550 cryostat (Thermo Scientific) and collected on Superfrost Plus slides (Menzel–Glaser). Four sections from both retinas were collected on the same slide.

Histology

Terminal deoxynucleotidyl transferase (TdT) mediated dUTP nick end labeling, or TUNEL, was used to assess apoptosis in retinal slices. Slides were treated using an In Situ Cell Death Detection Kit, Fluorescein (Roche) following the manufacturer's instructions for cryopreserved tissue. Positive and negative TUNEL control sections (DNAse I treated sections and sections without TdT) were included on each slide. Slides were then stained with 1 μM DAPI in PBS (GIBCO, pH 7.4). Fluoromount-G (Southern Biotech) was used to mount coverslips onto slides. Slides were imaged on an Olympus VS120 slide scanner through a 40× air objective using DAPI and FITC filters. Images were analyzed using ImageJ. Each section was broken up into 250×250 μm fields of roughly equal cell number, and three fields from each section were randomly chosen. Apoptotic cells were identified by colocalized DAPI and fluorescein signals. Thickness of nuclear layers was measured at four equidistant positions along the image and averaged. Retinal ganglion cells were counted over a 100 μm section. Two counts were made and averaged.

Open-Field Test

Rd1 mice were placed in a 190 × 100 mm circular chamber. The chamber was surrounded by six panels of 500 nm LEDs (Roithner Laserteknik), providing uniform illumination with a light intensity of 2.5×10^{16} photons/cm^2/sec. The mice were dark-adapted for 1 hour and habituated to the experimental chamber for 5 min prior to each experiment. Exploratory behavior was recorded using an IR sensitive video camera (Logitech C310) for 5 min in darkness under IR illumination, then the chamber was illuminated by the 500 nm LEDs, and mouse locomotion was monitored for an additional 5 min. The apparatus was cleaned after each experiment. Each mouse was tested once before intravitreal injection and again 6 hours after injection of either 20 mM DENAQ or sham. Videos were analyzed with motion tracking software (Tracker) to record the animals' velocity and position. The ratio of activity light / activity dark was defined as mean velocity in the light / mean velocity in darkness.

Visual Fear Conditioning Test

Fear conditioning was conducted in a 12 × 10 × 12 inch chamber with an electrified metal bar floor (Coulbourn Instruments). Prior to the experiment, animals were habituated by handling intervals interspersed over two days and with a 5 min exposure to the chamber. On day one, groups of WT mice, sham-injected *rd1* mice, or DENAQ-injected *rd1* mice (6 hours after intravitreal injection of 10 mM DENAQ or sham) were subjected to paired stimuli or unpaired stimuli. Paired conditioning consisted of a 5 min habituation period in the dark, followed by three 10 sec white light stimuli each co-terminating with a 2 sec foot shock, with 15 sec between light flashes. Unpaired conditioning was identical except the three foot shocks and three light stimuli were interleaved with 5–12 sec between stimuli. On day two the mice were tested for recall of the light-cued conditioning. The recall trial consisted of a 5 min habituation period in the dark followed by a 30 sec white light stimulus. The apparatus was cleaned after each experiment. Two house lights provided dim illumination (1×10^{13} photons/cm^2/sec) sufficient to allow video recording throughout the experiment, but below the threshold for DENAQ activation. The bright light cue was provided by two white LED arrays attached to the inner chamber ceiling (1.1×10^{15} photons/cm^2/sec). Locomotor activity was analyzed as in the open field assay.

Supplementary Material

Refer to Web version on PubMed Central for supplementary material.

Acknowledgments

We thank Lars Holzhausen and Natasha Slepak for help with experiments, Florian Huber for chemical synthesis and Nace Golding for insightful comments. This work was supported by grants to R.H.K. from the National Eye Institute (EY018957, P30 EY003176, and PN2 EY018241). R.H.K. and D.T. are SAB members and consultants of Photoswitch Bioscience, Inc., which is developing commercial uses for chemical photoswitches. I.T., V.D., and C.M.S. performed electrophysiological experiments. A.P. and N.G. performed histological experiments. I.T., A.F. and D.K. performed behavioral experiments. D.T. synthesized photoswitch compounds. R.V.G. provided useful advice. I.T. and R.H.K. designed the experiments and wrote the manuscript. R.H.K. supervised the project.

References

Amendola T, Fiore M, Aloe L. Postnatal changes in nerve growth factor and brain derived neurotrophic factor levels in the retina, visual cortex, and geniculate nucleus in rats with retinitis pigmentosa. Neuroscience letters. 2003; 345:37–40. [PubMed: 12809983]

Artigas JM, Felipe A, Navea A, Fandino A, Artigas C. Spectral transmission of the human crystalline lens in adult and elderly persons: color and total transmission of visible light. Investigative ophthalmology & visual science. 2012; 53:4076–4084. [PubMed: 22491402]

Bowes C, Li T, Danciger M, Baxter LC, Applebury ML, Farber DB. Retinal degeneration in the rd mouse is caused by a defect in the [beta] subunit of rod cGMP-phosphodiesterase. Nature. 1990; 347:677–680. [PubMed: 1977087]

Busskamp V, Duebel J, Balya D, Fradot M, Viney TJ, Siegert S, Groner AC, Cabuy E, Forster V, Seeliger M, et al. Genetic reactivation of cone photoreceptors restores visual responses in retinitis pigmentosa. Science. 2010; 329:413–417. [PubMed: 20576849]

Caporale N, Kolstad KD, Lee T, Tochitsky I, Dalkara D, Trauner D, Kramer R, Dan Y, Isacoff EY, Flannery JG. LiGluR restores visual responses in rodent models of inherited blindness. Molecular therapy : the journal of the American Society of Gene Therapy. 2011; 19:1212–1219. [PubMed: 21610698]

Chow BY, Han X, Dobry AS, Qian X, Chuong AS, Li M, Henninger MA, Belfort GM, Lin Y, Monahan PE, Boyden ES. High-performance genetically targetable optical neural silencing by light-driven proton pumps. Nature. 2010; 463:98–102. [PubMed: 20054397]

Martin DF, Maguire MG, Fine SL, Ying GS, Jaffe GJ, Grunwald JE, Toth C, Redford M, Ferris FL 3rd. Comparison of Age-related Macular Degeneration Treatments Trials Research, G. Ranibizumab and bevacizumab for treatment of neovascular age-related macular degeneration: two-year results. Ophthalmology. 2012; 119:1388–1398. [PubMed: 22555112]

Fischer E, Frankel M, Wolovsky R. Wavelength Dependence of Photoisomerization Equilibria in Azocompounds. The Journal of Chemical Physics. 1955; 23:1367–1367.

Fortin DL, Banghart MR, Dunn TW, Borges K, Wagenaar DA, Gaudry Q, Karakossian MH, Otis TS, Kristan WB, Trauner D, Kramer RH. Photochemical control of endogenous ion channels and cellular excitability. Nature methods. 2008; 5:331–338. [PubMed: 18311146]

Garcia-Amoros J, Diaz-Lobo M, Nonell S, Velasco D. Fastest thermal isomerization of an azobenzene for nanosecond photoswitching applications under physiological conditions. Angew Chem Int Ed Engl. 2012; 51:12820–12823. [PubMed: 23144016]

Hattar S, Lucas RJ, Mrosovsky N, Thompson S, Douglas RH, Hankins MW, Lem J, Biel M, Hofmann F, Foster RG, Yau KW. Melanopsin and rod-cone photoreceptive systems account for all major accessory visual functions in mice. Nature. 2003; 424:76–81. [PubMed: 12808468]

Humayun MS, Dorn JD, da Cruz L, Dagnelie G, Sahel JA, Stanga PE, Cideciyan AV, Duncan JL, Eliott D, Filley E, et al. Interim results from the international trial of Second Sight's visual prosthesis. Ophthalmology. 2012; 119:779–788. [PubMed: 22244176]

Hunter JJ, Morgan JI, Merigan WH, Sliney DH, Sparrow JR, Williams DR. The susceptibility of the retina to photochemical damage from visible light. Progress in retinal and eye research. 2012; 31:28–42. [PubMed: 22085795]

Jones BW, Kondo M, Terasaki H, Lin Y, McCall M, Marc RE. Retinal remodeling. Japanese journal of ophthalmology. 2012; 56:289–306. [PubMed: 22644448]

Khandhadia S, Cherry J, Lotery AJ. Age-related macular degeneration. Advances in experimental medicine and biology. 2012; 724:15–36. [PubMed: 22411231]

Kitamura E, Danciger M, Yamashita C, Rao NP, Nusinowitz S, Chang B, Farber DB. Disruption of the gene encoding the beta1-subunit of transducin in the Rd4/+ mouse. Investigative ophthalmology & visual science. 2006; 47:1293–1301. [PubMed: 16565360]

Ladas ID, Karagiannis DA, Rouvas AA, Kotsolis AI, Liotsou A, Vergados I. Safety of repeat intravitreal injections of bevacizumab versus ranibizumab: our experience after 2,000 injections. RETINA. 2009; 29:313–318. [PubMed: 19287287]

Lagali PS, Balya D, Awatramani GB, Munch TA, Kim DS, Busskamp V, Cepko CL, Roska B. Light-activated channels targeted to ON bipolar cells restore visual function in retinal degeneration. Nature neuroscience. 2008; 11:667–675.

Lamba DA, Gust J, Reh TA. Transplantation of Human Embryonic Stem Cell-Derived Photoreceptors Restores Some Visual Function in Crx-Deficient Mice. Cell Stem Cell. 2009; 4:73–79. [PubMed: 19128794]

Lee SC, Ishida AT. Ih Without Kir in Adult Rat Retinal Ganglion Cells. Journal of Neurophysiology. 2007; 97:3790–3799. [PubMed: 17488978]

Lewis AS, Chetkovich DM. HCN channels in behavior and neurological disease: Too hyper or not active enough? Molecular and Cellular Neuroscience. 2011; 46:357–367. [PubMed: 21130878]

Li YK, Wang F, Wang W, Luo Y, Wu PF, Xiao JL, Hu ZL, Jin Y, Hu G, Chen JG. Aquaporin-4 deficiency impairs synaptic plasticity and associative fear memory in the lateral amygdala: involvement of downregulation of glutamate transporter-1 expression. Neuropsychopharmacology : official publication of the American College of Neuropsychopharmacology. 2012; 37:1867–1878. [PubMed: 22473056]

Li ZY, Wong F, Chang JH, Possin DE, Hao Y, Petters RM, Milam AH. Rhodopsin transgenic pigs as a model for human retinitis pigmentosa. Investigative ophthalmology & visual science. 1998; 39:808–819. [PubMed: 9538889]

London NJ, Chiang A, Haller JA. The dexamethasone drug delivery system: indications and evidence. Advances in therapy. 2011; 28:351–366. [PubMed: 21494891]

Loo, D. In Situ Detection of Apoptosis by the TUNEL Assay: An Overview of Techniques. In: Didenko, VV., editor. DNA Damage Detection In Situ, Ex Vivo, and In Vivo. Humana Press; 2011. p. 3-13.

Marc RE, Jones BW, Watt CB, Strettoi E. Neural remodeling in retinal degeneration. Progress in retinal and eye research. 2003; 22:607–655. [PubMed: 12892644]

Milam AH, Li ZY, Fariss RN. Histopathology of the human retina in retinitis pigmentosa. Progress in retinal and eye research. 1998; 17:175–205. [PubMed: 9695792]

Mourot A, Kienzler MA, Banghart MR, Fehrentz T, Huber FM, Stein M, Kramer RH, Trauner D. Tuning photochromic ion channel blockers. ACS chemical neuroscience. 2011; 2:536–543. [PubMed: 22860175]

Mourot A, Tochitsky I, Kramer RH. Light at the end of the channel: Optical manipulation of intrinsic neuronal excitability with chemical photoswitches. Frontiers in Molecular Neuroscience. 2013; 6

Müller F, Scholten A, Ivanova E, Haverkamp S, Kremmer E, Kaupp UB. HCN channels are expressed differentially in retinal bipolar cells and concentrated at synaptic terminals. European Journal of Neuroscience. 2003; 17:2084–2096. [PubMed: 12786975]

Noell WK, Walker VS, Kang BS, Berman S. Retinal damage by light in rats. Investigative ophthalmology. 1966; 5:450–473. [PubMed: 5929286]

Petersen-Jones S. Advances in the molecular understanding of canine retinal diseases. The Journal of small animal practice. 2005; 46:371–380. [PubMed: 16119056]

Polosukhina A, Litt J, Tochitsky I, Nemargut J, Sychev Y, De Kouchkovsky I, Huang T, Borges K, Trauner D, Van Gelder RN, Kramer RH. Photochemical restoration of visual responses in blind mice. Neuron. 2012; 75:271–282. [PubMed: 22841312]

Postea O, Biel M. Exploring HCN channels as novel drug targets. Nat Rev Drug Discov. 2011; 10:903–914. [PubMed: 22094868]

Ren L, Liang H, Diao L, He S. Changing dendritic field size of mouse retinal ganglion cells in early postnatal development. Dev Neurobiol. 2010; 70:397–407. [PubMed: 19998271]

Roderick TH, Chang B, Hawes NL, Heckenlively JR. A new dominant retinal degeneration (Rd4) associated with a chromosomal inversion in the mouse. Genomics. 1997; 42:393–396. [PubMed: 9205110]

Sancho-Pelluz J, Arango-Gonzalez B, Kustermann S, Romero FJ, van Veen T, Zrenner E, Ekstrom P, Paquet-Durand F. Photoreceptor cell death mechanisms in inherited retinal degeneration. Molecular neurobiology. 2008; 38:253–269. [PubMed: 18982459]

Santoro B, Piskorowski RA, Pian P, Hu L, Liu H, Siegelbaum SA. TRIP8b Splice Variants Form a Family of Auxiliary Subunits that Regulate Gating and Trafficking of HCN Channels in the Brain. Neuron. 2009; 62:802–813. [PubMed: 19555649]

Schwartz SD, Hubschman JP, Heilwell G, Franco-Cardenas V, Pan CK, Ostrick RM, Mickunas E, Gay R, Klimanskaya I, Lanza R. Embryonic stem cell trials for macular degeneration: a preliminary report. Lancet. 2012; 379:713–720. [PubMed: 22281388]

Sekirnjak C, Jepson LH, Hottowy P, Sher A, Dabrowski W, Litke AM, Chichilnisky EJ. Changes in physiological properties of rat ganglion cells during retinal degeneration. J Neurophysiol. 2011; 105:2560–2571. [PubMed: 21389304]

Stacey PC, Raine CH, O'Donoghue GM, Tapper L, Twomey T, Summerfield AQ. Effectiveness of computer-based auditory training for adult users of cochlear implants. International journal of audiology. 2010; 49:347–356. [PubMed: 20380610]

Stasheff SF. Emergence of sustained spontaneous hyperactivity and temporary preservation of OFF responses in ganglion cells of the retinal degeneration (rd1) mouse. J Neurophysiol. 2008; 99:1408–1421. [PubMed: 18216234]

Stradleigh TW, Ogata G, Partida GJ, Oi H, Greenberg KP, Krempely KS, Ishida AT. Colocalization of hyperpolarization-activated, cyclic nucleotide-gated channel subunits in rat retinal ganglion cells. The Journal of Comparative Neurology. 2011; 519:2546–2573. [PubMed: 21456027]

Thyagarajan S, van Wyk M, Lehmann K, Lowel S, Feng G, Wassle H. Visual function in mice with photoreceptor degeneration and transgenic expression of channelrhodopsin 2 in ganglion cells. The Journal of neuroscience : the official journal of the Society for Neuroscience. 2010; 30:8745–8758. [PubMed: 20592196]

Weiland JD, Cho AK, Humayun MS. Retinal prostheses: current clinical results and future needs. Ophthalmology. 2011; 118:2227–2237. [PubMed: 22047893]

Wong KY, Dunn FA, Graham DM, Berson DM. Synaptic influences on rat ganglion-cell photoreceptors. J Physiol. 2007; 582:279–296. [PubMed: 17510182]

Wu X, Liao L, Liu X, Luo F, Yang T, Li C. Is ZD7288 a selective blocker of hyperpolarization-activated cyclic nucleotide-gated channel currents? Channels. 2012; 6:438–442. [PubMed: 22989944]

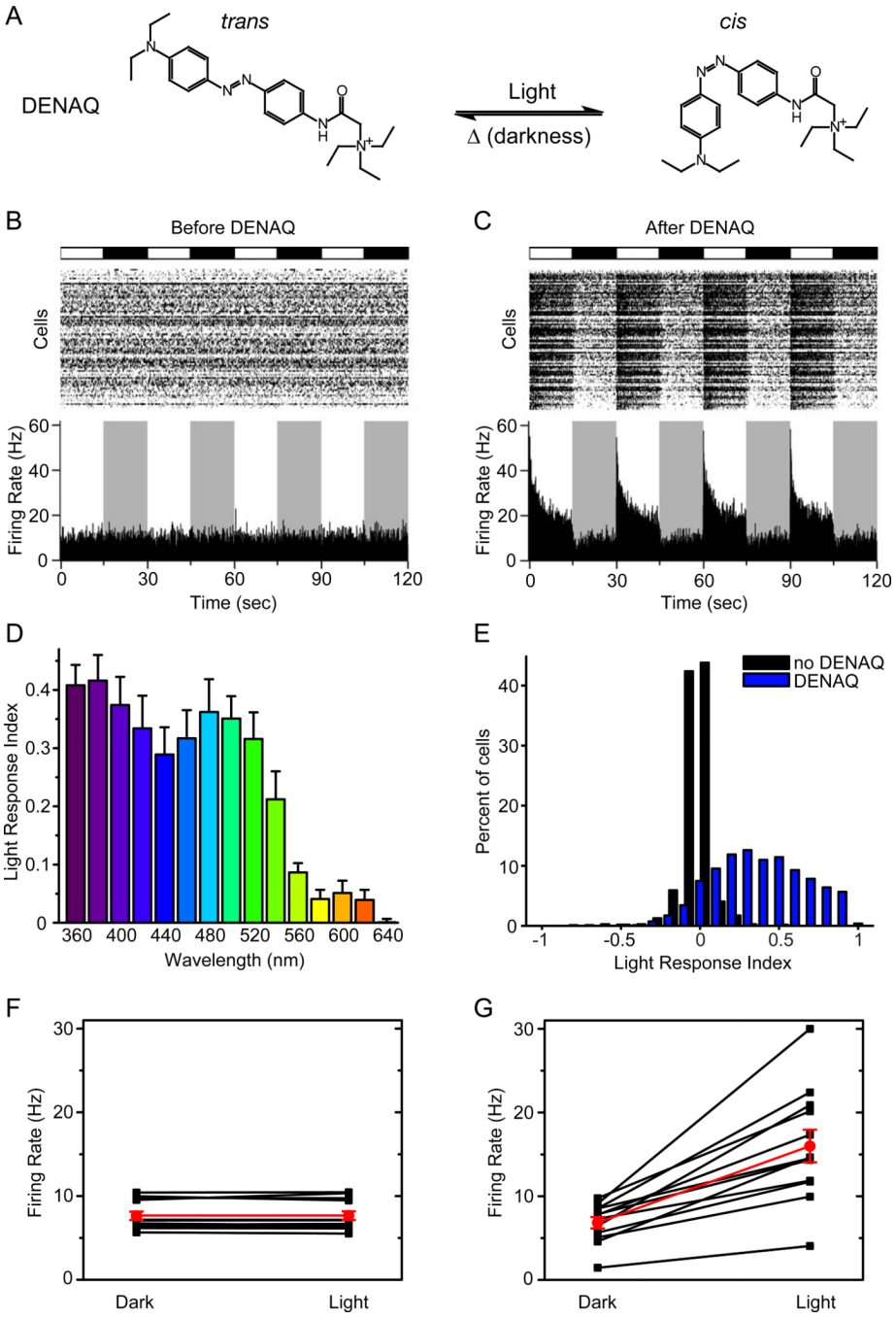

Figure 1. The red-shifted photoswitch DENAQ restores light responses to blind retinas from *rd1* mice

(**A**) Molecular structure of DENAQ. Light converts DENAQ from the *trans* to the *cis* form, and the compound quickly relaxes back to the *trans* form in the dark.

(**B–C**) MEA recording from an *rd1* retina before DENAQ treatment (**B**) and after treatment with 300 μM DENAQ (**C**). Light (white) and dark (black/gray) episodes are shown.

(**D**) Spectral sensitivity of the DENAQ-mediated light response.

(**E**) LRI value distributions for RGCs from untreated (black) (median LRI=0, n=12 retinas) and DENAQ-treated (blue) *rd1* retinas (median LRI=0.42, n=12 retinas, $p<0.001$, rank sum test).

(**F–G**) DENAQ restored light responses in every retina tested. Mean RGC firing rate for each retina in light and darkness before (n=12 retinas, p=0.94) (**F**) and after DENAQ treatment (n=12 retinas, p<0.001) (**G**). Mean±SEM values are shown in red.

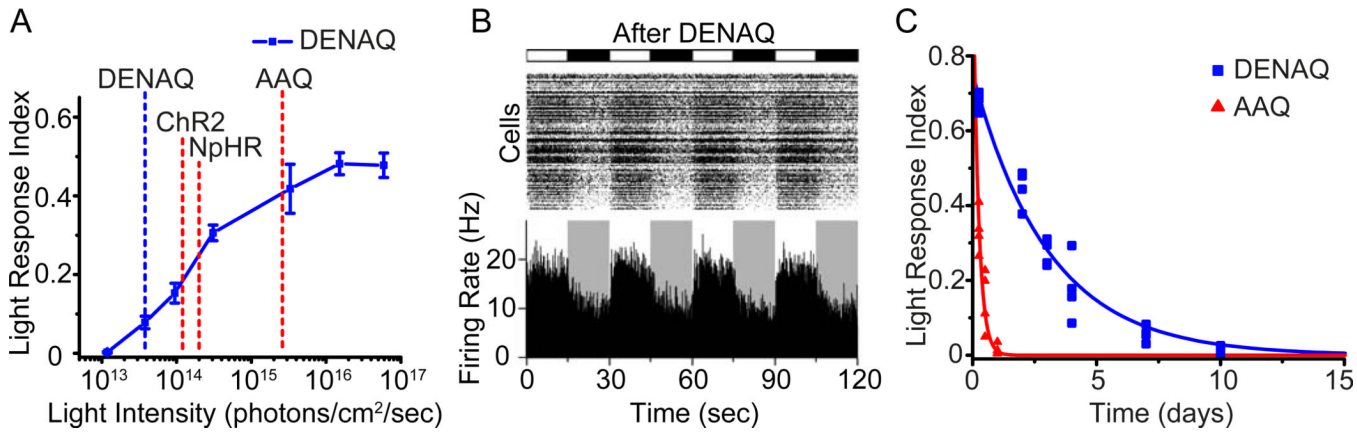

Figure 2. Intensity requirement for restoring light responses and persistence of DENAQ in the eye

(**A**) Light intensity vs. response curve for DENAQ (n=5 retinas). Data are mean±SEM. Labeled dotted lines represent the thresholds for activation of DENAQ (blue), ChR2 (Thyagarajan et al., 2010) (red), NpHR (Busskamp et al., 2010) (red) and AAQ (Polosukhina et al., 2012) (red) in the retina.

(**B**) MEA recording from a DENAQ-treated *rd1* retina stimulated with moderate intensity (3×10^{14} photons/cm^2/sec) white light. Light (white) and dark (black/gray) episodes are shown.

(**C**) Persistence of photosensitization elicited by *in vivo* injection of AAQ (red, half-life=3.6 hours) and DENAQ (blue, half-life=2.1 days). Responses were measured on the MEA *ex vivo*, hours to days after *in vivo* injection of 2 μL of 20 mM photoswitch (n=4 retinas per time point). Photoswitch half-life was calculated by fitting the data with a monoexponential decay function.

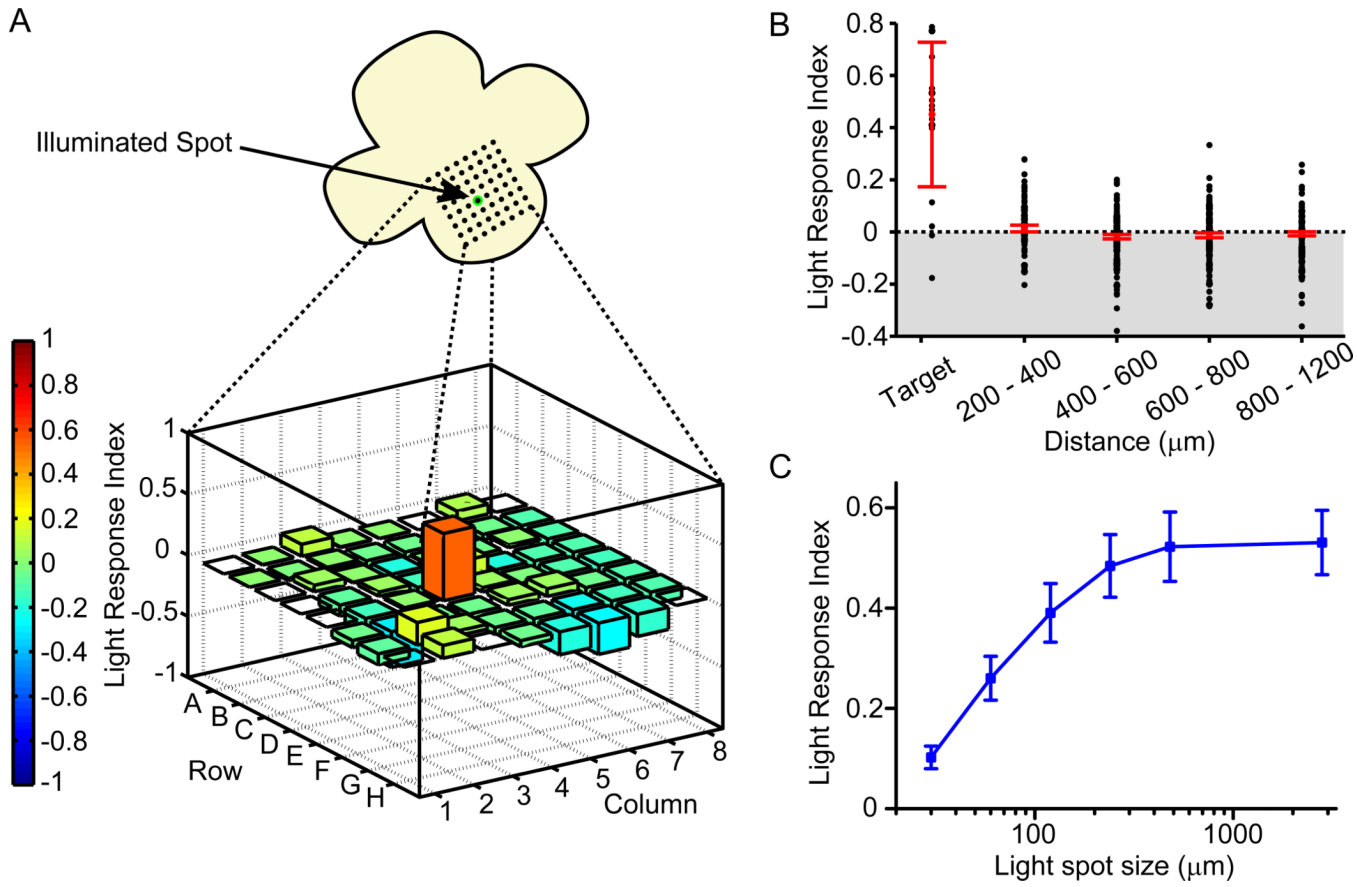

Figure 3. The DENAQ-treated *rd1* retina generates spatially precise light responses

(**A**) Targeted illumination of a portion of an *rd1* retina centered on a single MEA electrode (top). Electrode E4 was stimulated with a 60 μm diameter light spot. Only the targeted electrode recorded a large increase in RGC firing in response to white light (bottom). PI values are color-coded (scale at left) and also represented by bar height. The orange bar is electrode E4. Empty squares are electrodes on which no action potentials were recorded. (**B**) Targeted illumination elicits an increase in activity in stimulated RGCs and has no effect on surrounding RGCs (n = 16 cells and n = 741 cells, respectively, from seven retinas). LRI values of RGCs (black circles) as a function of distance from the target electrode, displayed in 200 μm bins. Median plus and minus the 95% confidence intervals are shown in red. (**C**) Responses of DENAQ-treated *rd1* RGCs to stimulation with spots of light of increasing diameter. The light response saturates at 240 μm diameter spot size. Data are mean±SEM, n=20 cells.

See also Table S1.

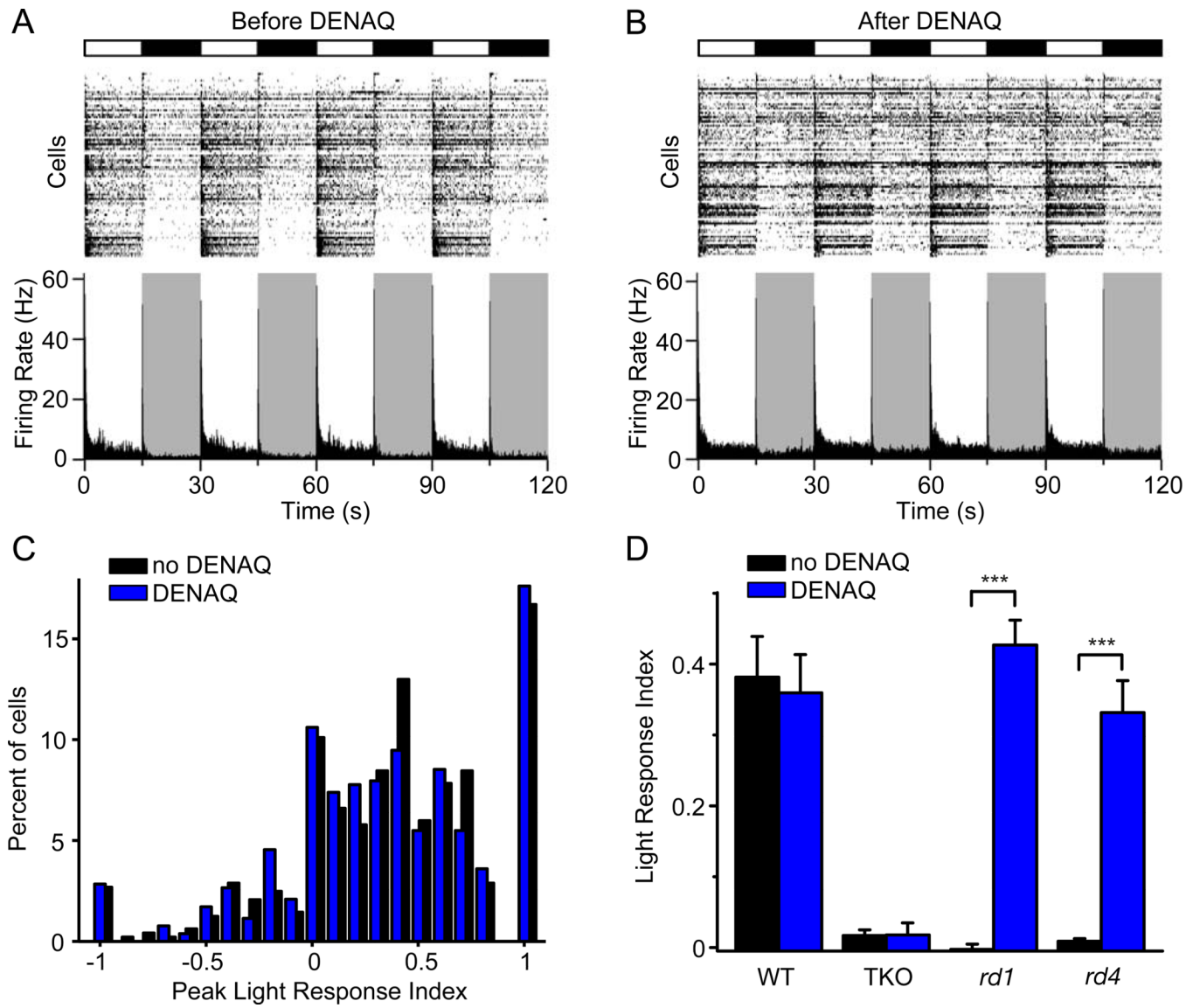

Figure 4. DENAQ only photosensitizes retinas in which rod and cone photoreceptors have degenerated

(**A**–**B**) MEA recording from a WT retina before (**A**) and after (**B**) treatment with 300 μM DENAQ. Light (white) and dark (black/gray) episodes are shown.

(**C**) RGC PLRI values for WT retinas before (black) and after (blue) DENAQ treatment (n=6 retinas, p=0.34, rank sum test).

(**D**) Light responses of untreated and DENAQ-treated WT (n=6, p=0.72), TKO (n=6, p=0.97), *rd1* (n=12, p<0.001) and *rd4* retinas (n=6, p<0.001). Mean PLRI values are shown for WT retinas and mean LRI values for TKO, *rd1* and *rd4* retinas. Data are mean±SEM.

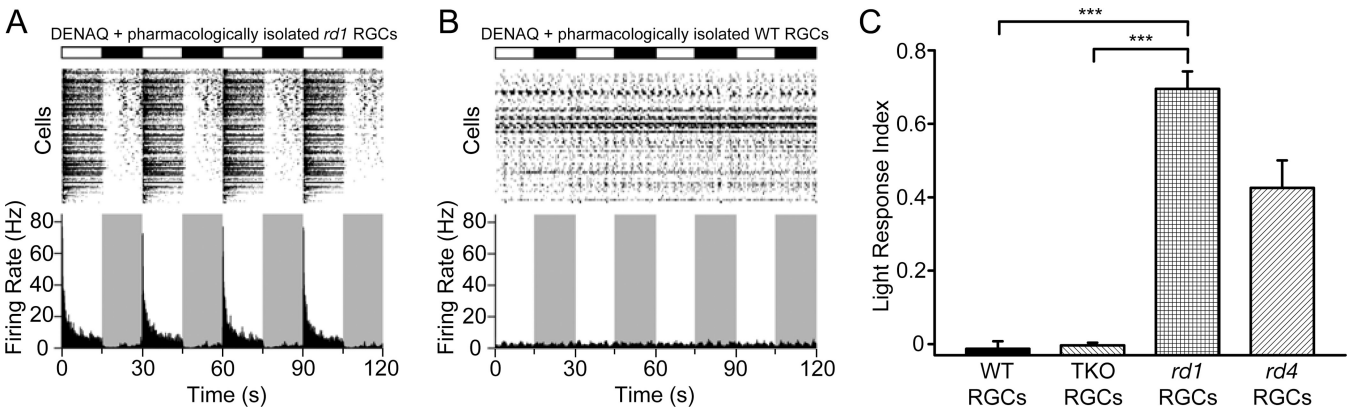

Figure 5. DENAQ selectively photosensitizes RGCs from retinas with degenerated photoreceptors

(**A–B**) MEA recording from pharmacologically isolated *rd1* (**A**) and WT (**B**) RGCs.

(**C**) Light responses of pharmacologically isolated WT RGCs (mean LRI=−0.01, n=10 retinas, $p<0.001$), TKO RGCs (mean LRI=0, n=6 retinas, $p<0.001$), *rd1* RGCs (mean LRI=0.70, n=8 retinas) and *rd4* RGCs (mean LRI=0.43, n=6 retinas).

See also Figures S1 and S2.

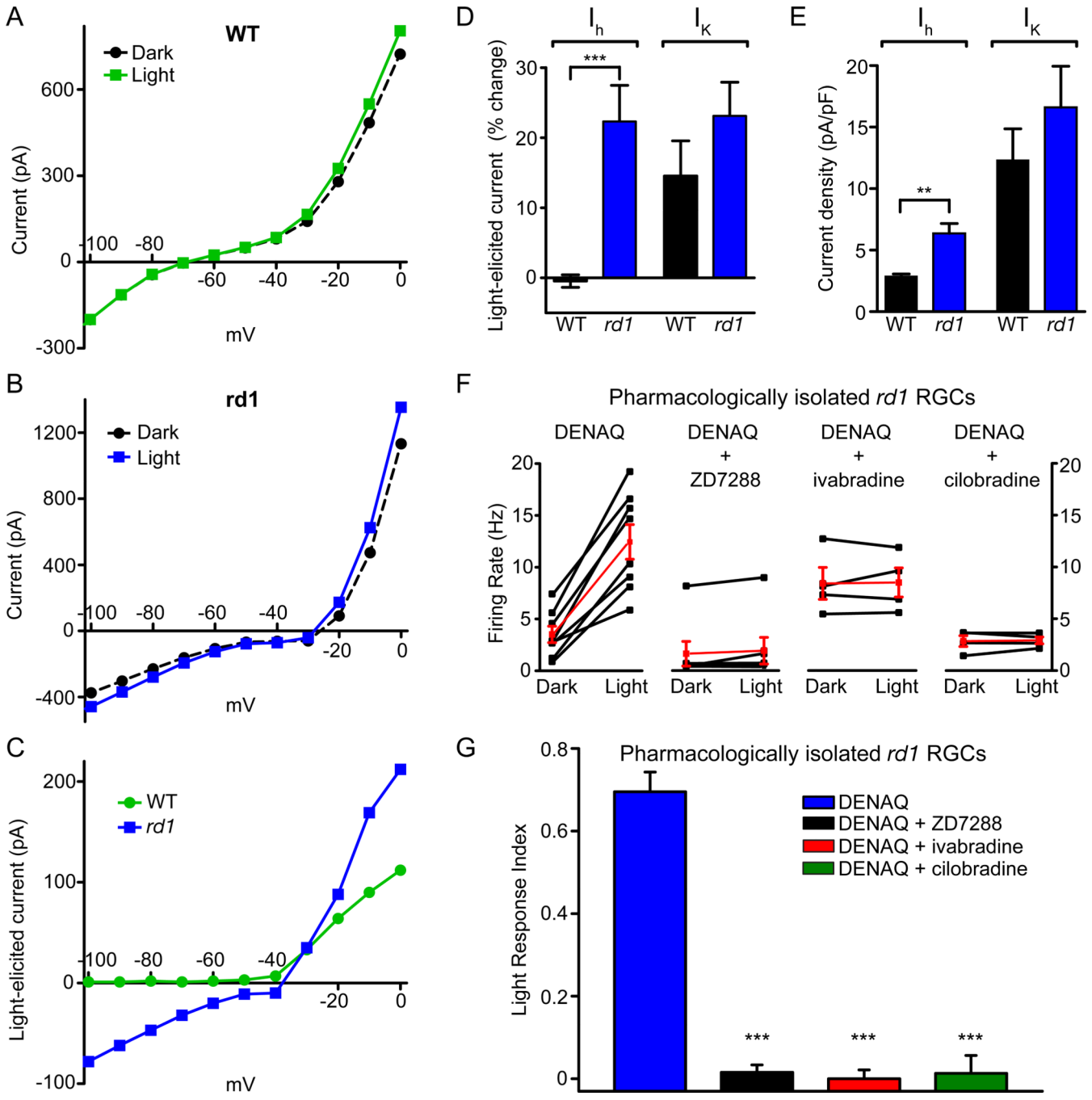

Figure 6. DENAQ selectively photosensitizes I_h in *rd1* but not WT RGCs

(**A–B**) Current vs. voltage relationships of RGCs from WT (**A**) and *rd1* (**B**) retinas obtained in darkness (black) or in light (green or blue).

(**C**) Light-elicited current, defined as the difference between currents measured in light and dark in the WT RGC (from panel **A**) (green) and in the *rd1* RGC (from panel **B**) (blue).

(**D**) Light-elicited change in I_h (left), and in I_K (right) in WT RGCs (black) (n=11) and in *rd1* RGCs (blue) (n=9), shown as percent difference. I_h was photoregulated in *rd1* (mean=22%) RGCs, but not in WT RGCs (mean=−0.3%, $p<0.001$). I_K was photosensitized to the same extent in WT and *rd1* RGCs (WT mean=15%, *rd1* mean=23%, $p=0.2$).

(**E**) I_h and I_K current densities in WT (black) (n=13 cells) and *rd1* (blue) (n=7) RGCs. I_h density was significantly higher in *rd1* RGCs (mean=6.4 pA/pF) than in WT RGCs (mean=2.9 pA/pF, $p<0.01$). I_K density was not significantly different (WT mean=12.3 pA/pF, *rd1* mean=16.6 pA/pF, p=0.3).
(**F**) DENAQ treatment photosensitizes *rd1* RGCs (n=8 retinas, mean firing rate increase (MFRI)=3.5×, $p<0.001$) (left). Subsequent application of I_h blockers - ZD7288 (n=7 retinas, MFRI=1.18, p=0.38) (second from left), ivabradine (n=4 retinas, MFRI=1.01, p=0.87) (second from right) or cilobradine (n=4 retinas, MFRI=1.02, p=0.81) (right) abolishes DENAQ-mediated *rd1* RGC photosensitization. Mean±SEM firing rates are shown in red.
(**G**) Mean light response index of DENAQ-treated *rd1* RGCs (mean LRI=0.7) (blue). I_h blockers - ZD7288 (mean LRI=0.02, $p<0.001$) (black), ivabradine (mean LRI=0, $p<0.001$) (red) and cilobradine (mean LRI=0.01, $p<0.001$) (green) eliminate DENAQ-mediated RGC photosensitization. Data are mean±SEM.
See also Figures S3 and S4.

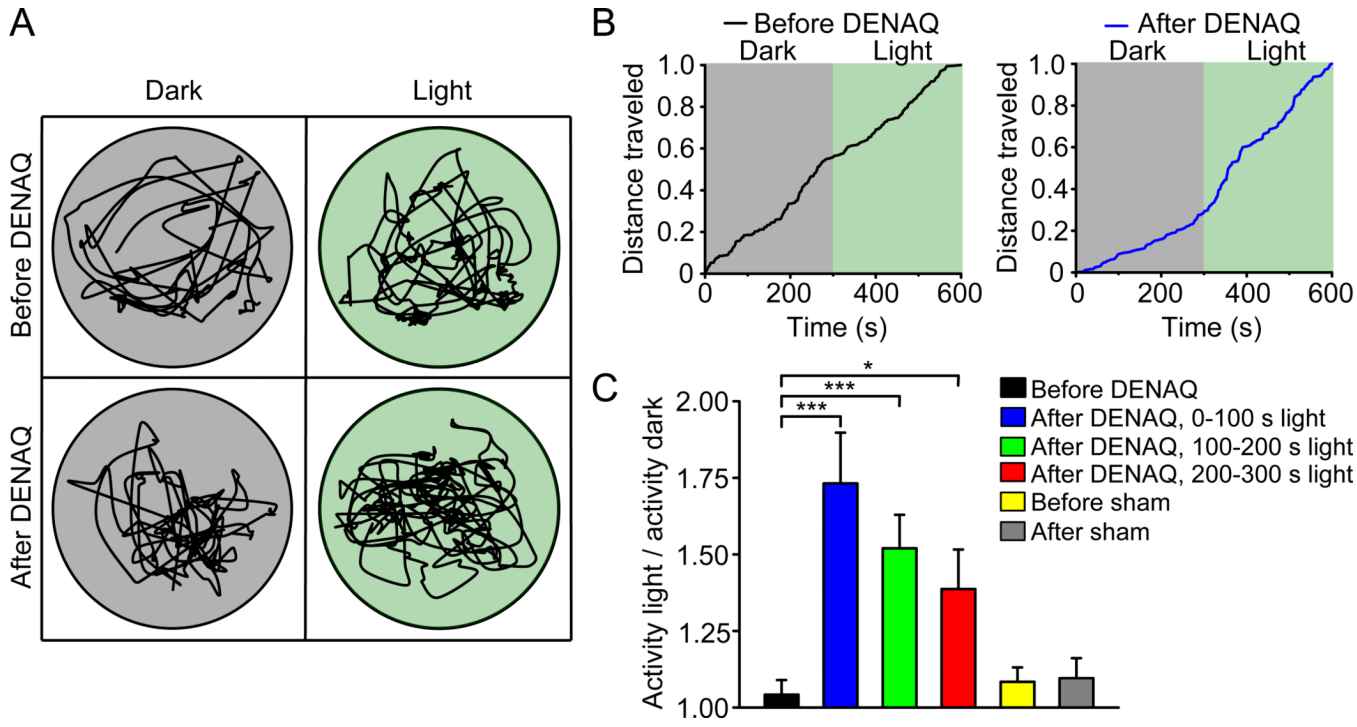

Figure 7. DENAQ restores light-modulated open field locomotor behavior in blind mice

(**A**) Movement trajectory of the same *rd1* mouse exploring an open cylindrical cage in the dark (gray) and under 500 nm light (green) before (top) and after (bottom) DENAQ injection.

(**B**) Cumulative distance traveled by an *rd1* mouse before (left) and after (right) DENAQ injection.

(**C**) Bar graph of activity in the light divided by activity in darkness before (black) (n=20 mice, mean=1.04) and after intravitreal injection of DENAQ and before (yellow) or after (gray) sham injection (n=6 mice, p=0.88). Activity ratios for the first 100 sec of exploratory behavior of DENAQ-injected mice (blue) (mean=1.73, p<0.001), 100–200 sec in the light (green) (mean=1.52, p<0.001) and the final 100 sec in the light (red) (200–300 sec) (mean=1.39, p<0.05). The amount of exploratory activity decreased with time. Data are mean±SEM.

See also Figure S5.

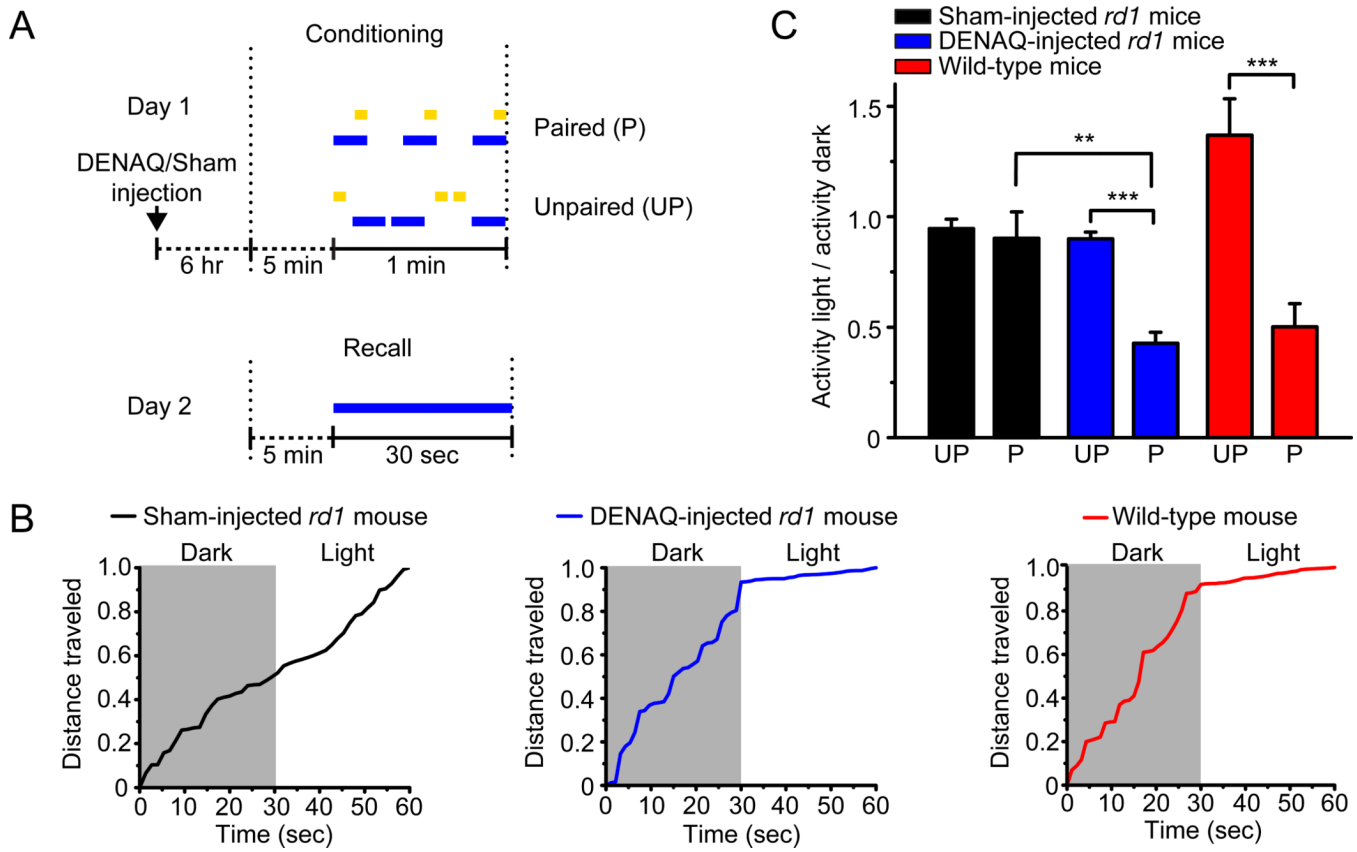

Figure 8. DENAQ enables visual learning in blind mice

(**A**) Diagram of the paired, unpaired conditioning and recall protocols for the visual fear conditioning assay. Electric foot shock (yellow) and light flash (blue) episodes are shown.

(**B**) Cumulative distance traveled by a paired-conditioned sham-injected *rd1* mouse (left, black), a paired-conditioned DENAQ-injected *rd1* mouse (middle, blue) and a paired-conditioned WT mouse (right, red) in the 30 sec of darkness preceding the light flash and the subsequent 30 sec in the light during the recall trial.

(**C**) Bar graph of activity in light divided by activity in darkness for sham-injected *rd1* (n=9, p=0.71), DENAQ-injected *rd1* (n=10, p<0.001) and WT mice (n=10, p<0.001) during the recall trial. Data are mean±SEM.